LuxS-mediated AI-2 signaling regulates chemotaxis, flagellar motility, and virulence genes in *Salmonella Typhimurium* and contributes to colonization in the murine gut

Anmol Singh[a], Abhilash Vijay Nair[a,d], R. S. Rajmani[c], Dipshikha Chakravortty[a,c]*

[a]Department of Microbiology and Cell Biology, Division of Biological

[b]Molecular Biophysics Unit, Indian Institute of Science, Bengaluru, India

[c]Adjunct Faculty, School of Biology, Indian Institute of Science Education and Research, Thiruvananthapuram, India

[d]Present address: Department of Microbiology and Immunology, Vagelos College of Physicians and Surgeons, Columbia University, New York, NY 10032, USA

*Corresponding author: dipa@iisc.ac.in,

Tel: +91 80 2293 2842,

Fax: +91 80 2360 2697

Abstract

The coordinated response through AI-2 allows *Salmonella* to adapt to its environment and regulate virulence factors, biofilm formation, Motility, and other behaviors crucial for survival and infection. Understanding these mechanisms is essential for developing strategies to interfere with *Salmonella's* ability to cause disease. In this study, we demonstrate that AI-2 signaling modulates the transcription of genes involved in chemotaxis and flagellar Motility, thereby facilitating epithelial cell attachment and invasion in vitro and effective colonization in a murine infection model. We identify HilD, a master regulator of *Salmonella* pathogenicity island 1 (SPI-1) and motility genes, which was significantly downregulated in the absence of LuxS/AI-2 signaling, highlighting a central role for AI-2 in orchestrating virulence gene networks. Furthermore, LuxS/AI-2 signaling enhances resistance to host antimicrobial peptides and promotes intracellular survival by modulating the *pmrD/pmrAB* system. Transcriptomic analyses confirm that AI-2 influences multiple gene networks critical for *Salmonella* pathogenesis. *In vivo* studies reveal that disruption of AI-2 signaling impairs organ colonization, and co-treatment with AI-2 inhibitors and antibiotics reduces bacterial virulence, suggesting a promising therapeutic strategy. Together, our findings uncover a multifaceted regulatory role of AI-2 signaling in modulating *Salmonella Typhimurium* motility, immune evasion, and pathogenesis.

Introduction

Bacteria were initially thought to be solitary microbes that led an independent life cycle of multiplying and increasing their numbers, and some of them could cause life-threatening infections. However, a series of discoveries led to unravelling the mode of communication in these little beings referred to as quorum sensing (1-3). This process involves the production and secretion of chemical signals that are sensed by the neighbouring cells in the bacterial community and orchestrate a myriad of genes and pathways, resulting in coordinated behaviours such as adaptation, virulence and other critical community behaviours underscoring the advantages of communal living among bacterial populations (4, 5). Bacterial pathogenesis is very well governed by this communication paradigm. The pathogen, upon entry into the host, has to decide to stay and colonise, or utilise the host nutrients and run or employ all its virulence strategies without worrying about the repercussions. Interestingly, the community communicates, coordinates and makes the decision on the microbial pathogenesis (6, 7). Bacterial pathogens are the sole cause of serious bacterial infections (SBIs) worldwide, with an estimated 7.7 million deaths globally, with a rise in antimicrobial resistance, which further worsens the situation(8). *Salmonella* enterica serovar Typhimurium (STM) is a prominent etiological agent of foodborne illnesses and a leading contributor to non-typhoidal salmonellosis (NTS)(9). It faces very long odds while seeking to colonise and breach the intestinal barrier, including acidic pH, limited nutrient availability, bile salt toxicity, and competition from gut

59 microbiota. It is critical for the bacteria to establish and increase in number,
60 reaching the infectious dose to invade the host epithelial cells. Upon breaching
61 the epithelial barrier, it is engulfed by macrophages in the lamina propria,
62 facilitating its systemic dissemination throughout the host (10-13). With the
63 fluctuations of extreme conditions, *Salmonella* needs to be adept at sensing,
64 responding, and adapting to unprecedented situations.

65 *Salmonella* uses the autoinducer-2 (AI-2) chemical messenger for their
66 communication. This intercellular communication, called quorum sensing,
67 enables *Salmonella* to regulate and synchronize their behaviors when present at
68 high cell densities(14-16). The AI-2 in *S*. Typhimurium is a byproduct of the
69 activated methyl cycle (AMC), where initially, the S-adenosyl methionine(SAM)
70 is converted into S-adenosylhomocysteine(SAH) by methyl transferases (17).
71 The SAH is subsequently converted to the precursor of AI-2 molecule 4,5
72 dihydroxy-2,3-pentanedione (DPD) by the enzymes Pfs and LuxS,
73 respectively(18). Finally, DPD molecules autocyclize into (2R,4S)-2-methyl-
74 2,3,3,4-tetrahydroxytetra-hydrofuran (AI-2) molecules(19, 20).

75 Although the LuxS/AI-2 quorum-sensing signaling pathway is well
76 characterized, its physiological significance remains only partially understood in
77 *Salmonella* pathogenesis despite being a thoroughly established system. Studies
78 suggest that *Salmonella* quorum sensing regulates virulence, biofilm formation,
79 Motility, and antimicrobial resistance by regulating *Salmonella* Pathogenicity

80 Island-1, flagella, and antioxidative genes(21-23). Further, there is evidence of
81 involvement of AI-2 in Motility and chemotaxis in the Ag43-dependent
82 aggregation of *E. coli* and its roles in *E. coli* gut colonization(24). The study also
83 shows that chemotaxis towards self-produced AI-2 provides *E. coli* a fitness
84 advantage during gut colonization, hinges on fructoselysine metabolism(25). AI-
85 2, a molecule produced and detected by numerous bacterial species, has also been
86 found to be mimicked and synthesized by eukaryotic cells(26). Research has
87 demonstrated that several bacterial species exhibit a chemotactic response to AI-
88 2, highlighting its crucial role in forming intricate multispecies communities(27).
89 Notably, AI-2 is thought to influence the bacterial community structure in the
90 mammalian gut following antibiotic-induced dysbiosis and to bolster
91 colonization resistance against specific enteric pathogens(28). Thus, it is apparent
92 that *Salmonella* communication is a key to its pathogenesis. Despite these
93 findings, significant gaps remain in understanding the advantages of communal
94 living and how AI-2 signaling benefits *Salmonella* in physiologically relevant
95 conditions.

96 In our present study, we elucidate that the LuxS/AI-2 signaling cascade governs
97 the processes of the initial attachment and invasion into intestinal epithelial cells
98 *in vivo* in mice and *in vitro* by regulating chemotaxis and flagellar Motility.
99 Furthermore, LuxS/AI-2 signaling assists in intracellular survival by regulating
100 the *pmrABC* operon, which provides resistance against antimicrobial peptides. As

101 an alternative approach, inhibition of AI-2 signaling in combination with
102 antibiotics reduced *Salmonella* organ burden and delayed mortality in mice
103 models. We investigated the underlying mechanism of bacterial communal living
104 and communication, driving key stages of *Salmonella* pathogenesis within the
105 host.

106 **Materials and Methods**

107 **Bacterial strains and Growth conditions-**

108 The wild-type *Salmonella* enterica serovar Typhimurium strain 14028S (STM
109 WT), generously provided by Professor Michael Hensel from the Max Von
110 Pettenkofer-Institute for Hygiene and Medical Microbiology in Germany, was
111 employed in all experiments of this study. Bacterial strains were revived on LB
112 agar, with or without antibiotics, and LB broth cultures of wild-type, knockout,
113 and complemented strains were incubated at 37°C (170 rpm) using an orbital
114 shaker. Wherever necessary, antibiotics were used, including Kanamycin (50
115 µg/ml), Chloramphenicol (25 µg/ml), and Ampicillin (50 µg/ml).

116 **Bacterial gene knockout and strain generation**

117 *Salmonella enterica* serovar Typhimurium strain 14028 and isogenic mutants
118 were used for all experiments. *luxS*, *lsrB*, *lsrK,* and *lsrR* gene knockout and *luxS*
119 complement strains were made in our previous study **(S Table 1)**. Briefly, all the
120 knockout generation was done as described previously in one gene step

121 chromosomal gene inactivation method demonstrated by Datsenko and Wanner
122 (29).

123 Briefly, for the complement strain, the double-digested PCR amplified purified
124 *luxS* gene (containing BamH1 and HindIII restriction site sequences) was used to
125 clone in double-digested pQE-60. The respective ligated vector was transformed
126 into the STM Δ*luxS* strains to generate the complement strains. For the reporter
127 plasmid *plsr*-GFP generation, 256 bp of upstream of *lsrA* were cloned into the
128 promoter less vector pUA66. Finally, reporter plasmid transformed into the STM
129 WT and STM Δ*luxS*.

130 **Cell culture and maintenance**

131 Caco-2 epithelial cell lines were maintained in Dulbecco's Modified Eagle
132 Medium (DMEM, Lonza), supplemented with 10% FBS (Gibco), 1% non-
133 essential amino acids, 1% sodium pyruvate, and 1% penicillin-streptomycin
134 (Sigma-Aldrich) in a humidified incubator with 5% CO2 at 37 °C. The cells were
135 seeded into the respective cell culture plates for each experiment to conduct
136 intracellular survival assays and intracellular gene expression experiments.

137 **Gentamicin protection assay**

138 Caco-2 cells were seeded in tissue culture plates for infection. Cells were infected
139 with STM WT, STM Δ*luxS,* STM Δ*lsrB,* STM Δ*lsrK,* STM Δ*lsrR,* and
140 *STMΔluxS:luxS* (log phase culture growing overnight in LB broth). The
141 multiplicity of Infection (MOI) 20 was used for the intracellular survival assay

142 and *Salmonella* gene expression study (qRT-PCR). Following the infection of
143 STM strains into the cell line, the plate was spun for 5 minutes at 600 rpm using
144 a Rota-Superspin R–NV swing bucket centrifuge. After that, the plate was
145 incubated for 25 minutes at 37 °C with 5% CO_2 in a humidified incubator. Then,
146 the infected cells were washed with 1X PBS twice and treated with a 100 µg/ mL
147 concentration of gentamycin. After 1 hour, the media were changed with a
148 reduced concentration of gentamycin (25 µg/ mL) and incubated until time point.
149 The time points 2h, 6h, and 16h were taken for the qRT-PCR sample and 2h and
150 16h for the intracellular survival assay.

151 DPD supplementation (of 25 µM, 50 µM,100 µM, and 200µM DPD) or spent
152 media of STM WT collected at 3h in LB growing treated STM Δ*luxS,* and
153 LuxS/AI-2 signaling inhibition(30, 31), the inhibitor (Z)-4- bromo-5-(
154 bromomethyllene)-3-methylfran-2(5H), known as BF-8 treatment, was given to
155 the STM WT culture, which was used for the gentamycin protection assay to
156 study the adhesion, invasion, and intracellular proliferation of STM.

157 **Invasion and intracellular survival assay**

158 The cells were lysed with 0.1% triton-X 100 in PBS at specific time points post-
159 infection. For the invasion, CFU was determined at 2h post-infection samples
160 and CFU in pre-inoculum. Percent invasion was calculated by using the formula-
161 [CFU at 2 hours]/ [CFU of pre-inoculum] ×100**.** For the fold proliferation, CFU

162 was determined at 2h and 16h post-infection samples. Fold proliferation was
163 determined using the formula [CFU at 16 hours]/ [CFU at 2 hours].

164 **Adhesion assay**

165 Adhesion assay was done as gentamycin protection assay with modification.
166 Infections were given to Caco-2 cells at MOI 20 and incubated for 10 minutes at
167 37 °C in a humidified incubator with 5% CO2. Thereafter, washing with 1X PBS
168 twice to eliminate any loosely adherent bacteria. After lysing the mammalian
169 cells with 0.1% Triton-X 100, samples were taken to release the bacteria into the
170 sample. After the collected samples were plated on LB agar plates at the
171 appropriate dilutions and incubated at 37 °C, the CFUs were enumerated. The
172 following formula was used to calculate the percentage adhesion = [(CFU at 10
173 min post-infection)/(CFU of the pre-inoculum)]× 100.

174 ***In vitro* motility assay-**

175 2 µl of bacterial culture was spotted onto the agar plates supplemented with 1%
176 casein enzyme hydrolysate, 0.5% yeast extract, 0.5% NaCl, and 0.5% glucose
177 with 0.3 % agar (swim agar plates) and 0.5% agar plates (swarm agar plates). The
178 swim agar plates were incubated at 37˚C for 6h, and swarm agar plates were
179 incubated for 12h. The diameters of the motility halos were measured at least
180 three angles of three replicate plates, and then images were taken using a BioRad
181 chemidoc.

182 **Chemotaxis assay-**

183 Chemotaxis assay was done by using μ-Slide Chemotaxis, ibidi. μ-Slide consists
184 of two distinct opposing liquid chambers or reservoirs separated by a small liquid
185 transition zone of 1 mm. Overnight grown STM WT, STM Δ*luxS*, and STM Δ*lsrB*
186 were followed by two washes with motility buffer (MB; 10 mM KPO4, 0.1 mM
187 EDTA, and 67 mM NaCl, pH 7), and then resuspension to a final OD600 to 0.3
188 in MB supplemented with 3.5% glucose (MBg)(24). To reduce metabolic
189 activity, cells were chilled for 20 minutes. A motility buffer was applied to the
190 transition zone. The first reservoir was completely filled with the bacterial cell
191 suspension, the second reservoir with STM WT spent media (Collected at 3h of
192 LB growth), synthetic DPD molecule, and the known chemoattractant L-serine.
193 In a different experiment, the numbers of bacteria that transmigrated from the first
194 reservoir into the second reservoir were quantified by CFU analysis and bright
195 field microscopy (Leica microscope SP8 falcon, 63X).

196 **RNA isolation and RT-qPCR**

197 For the gene expression study in Luria Bertani (LB) media, overnight-grown
198 culture in LB media was subjected to a subculture (at 1:100) in LB. At 3h, 6h,9h,
199 and 12h, bacterial cell pellets were collected in TRIzol (from TaKaRa, RNA
200 isoPlus- 9109) and kept at -80˚C. Total RNA was isolated by chloroform
201 extraction followed by Isopropanol precipitation. To evaluate the quality, the
202 amount of RNA was quantified in nano drops and examined on a 2% agarose gel.
203 To produce cDNA, 2 μg of RNA sample was treated with DNase I at 37˚C for 1

204 hour (TaKaRa), followed by heating for 10 minutes at 65˚C. Then, DNA-free
205 RNA samples were used to make cDNA by using the PrimeScript RT reagent Kit
206 provided by TaKaRa (Cat# RR037A).
207 The gene expression of *Salmonella* upon Infection in Caco-2 infection was given
208 at MOI 20. At 2h, 6h, and 16h post-infection, samples were collected in TRIzol
209 (from TaKaRa, RNA isoPlus- 9109) and kept at -80˚C. Total RNA isolation and
210 cDNA were synthesized using a similar protocol described in the kit provided,
211 TRIzol (from TaKaRa, RNA isoPlus-9109) and TaKaRa (Cat# RR037A)
212 reagents according to the manufacturer's protocol. The list of expressions Primer
213 is provided in **S Table 2**. Quantitative PCR was carried out using a SYBR Green
214 Q-PCR kit (Takara), and the ΔΔCt method was used for quantification.

215 **RNA sequencing and analysis**

216 Bacteria were grown till mid-log phase and RNA extraction was performed using
217 Qiagen RNeasy Mini kit (Cat. No. 74104) with a few modifications. The RNA
218 samples were quantified on Nanodrop and Qubit flurometer using appropriate
219 standards. Appropriate dilutions were loaded on a High sensitivity RNA screen
220 tape and run on Agilent Tape station 4200 to determine the RNA integrity number
221 (RIN). For Library preparation, 1000ng of RNA sample was used for
222 ribodepletion by using NEB Next rRNA depletion kit Bacteria (Cat. no. NEB
223 E7850X), which includes Probe hybridization of RNA, RNase H digestion,
224 DNase 1 digestion according to the manufacturer's protocol. The NEBNext®

225 Ultra II Directional RNA Library prep kit for Illumina (Cat. no. E7760L), was
226 used to construct double-stranded cDNA libraries from the rRNA depleted RNA,
227 using RNA fragmentation, first strand cDNA synthesis with random primers,
228 second strand cDNA synthesis, end repair of double stranded cDNA, adapter
229 ligation, removal of excess adapter using sample purification beads, PCR
230 enrichment of adapter ligated DNA and clean-up of PCR products as instructed
231 by the manufacturer. The cleaned libraries were quantified on Qubit®flurometer
232 and appropriate dilutions loaded on a D1000 screen tape to determine the size
233 range of the fragments and the average library size.

234 The original raw data from the Illumina platform is transformed into sequenced
235 reads by base calling. Raw data are recorded in a FASTQ file containing sequence
236 information (reads) and corresponding sequencing quality information. The
237 quality of the reads was assessed using Fast QC v 0.11.9 before proceeding with
238 the downstream analysis(32). The reads were passed through SortMeRNAv4.3.7
239 (33) and were used against all eight rRNA databases provided to filter and remove
240 rRNA reads. The trimmed reads were then passed through fastp (34) to remove
241 adaptors, low-quality bases (Q< 36 bp). For mapping and quantification,
242 *Salmonella* Typhimurium 14028s reference genome and annotation were
243 downloaded from (https://ftp.ncbi.nlm.nih.gov/genomes/all/GCF/000/022/165/
244 GCF_000022165.1_ASM2216v1/). HISAT2 (35) was used to create the reference
245 index, and the trimmed & filtered reads were mapped to the indexed genome

using HISAT2. Quantification was performed with feature Count (36). A total of 4728 features were assigned in the raw count file. The raw count file is made into raw counts for individual sets, and the rest of the differential analysis is done according to the sets. The library sizes are plotted for individual sets. The transcripts with low read counts (< count of at least 10 for a minimum of 2 samples) were removed. The filtered read counts were normalized by transforming to the rlog transformation function (rlog) of DESeq2 (37) and are used for further analysis. Differential gene expression was analysed using the DESeq function from the DESeq2 package with a false discovery rate (FDR) cut-off of ≤ 0.05 and a minimum expression log2-fold change (FC) of ≥ 2/1. The counts are illustrated with a volcano plot. The top genes with the largest log2fold change are plotted as a heatmap.

Transmission electron microscopy

Flagella were visualized using the protocol described previously(38, 39). Briefly, overnight bacterial cultures were subcultured in LB media and incubated until it reached an OD of 0.1. During the subculture, STM WT was treated with AI-2 signaling inhibitor BF-8, and STM Δ*luxS* with STM WT spent media and synthetic DPD. The bacterial cultures were centrifuged at 2000 rpm for 10 min at 4◦C. The bacterial cells were washed with 1XPBS twice, and finally, the cells were resuspended in 100 µl of 1X PBS. 10 µl of the cell suspension was added

266 on a copper grid, air dried, stained with 1% uranyl acetate for 30 s, and visualized
267 under a transmission electron microscope (Thermo-Fischer Scientific).

268 **Immunofluorescence**

269 After appropriate post-infection incubation time in the adhesion assay, the media
270 was removed, and the cells were washed with 1X PBS and fixed with 3.5%
271 Paraformaldehyde for 10 min. The cells were then washed with 1X PBS,
272 incubated with the required rabit-raised anti-*Salmonella* primary antibody in a
273 buffer containing 2% BSA, and incubated for 1 hour at room temperature or
274 overnight at 4°Cmin. After washing with 1X PBS, the secondary antibody tagged
275 to a fluorochrome was added and incubated. For Caco-2 epithelial cells, FM464
276 dye was used. The coverslips were washed with PBS, mounted on a clean glass
277 slide using mounting media containing an anti-fade reagent, and observed under
278 the confocal microscope (Leica microscope SP8 falcon, at 63X oil immersion).

279 Mice intestine histochemistry samples were incubated with the required rabbit-
280 raised anti-*Salmonella* primary antibody in a buffer containing 0.01% saponin
281 and 2% BSA, and incubated for 1 hour at room temperature or overnight at
282 4°Cmin. After washing with 1X PBS, the secondary antibody tagged to a
283 fluorochrome was added and incubated for 1h at room temperature. The dye
284 DAPI was used to stain the intestinal nucleus. 40X oil immersion was used to
285 study the mice intestine histopathology (Zeiss 710 microscope, at 63X oil
286 immersion).

287 **Polymyxin treatment and survival assay**

288 Polymixin MIC was determined by using microbroth dilution methods.
289 Polymixin treatment (sub-MIC concentration 0.5 µg/ml) was given to the
290 overnight STM strains (10^7 cfu) in LB media. At 3h post-treatment, CFU was
291 determined by spread plate methods. For the time-dependent survival assay, we
292 collected the treated sample at 3h, 6h, 9h, and 12h and calculated the CFU. For
293 the mRNA expression study, samples were collected during mid-log phase (6h)
294 in Trizol and kept at -80°C for further RNA isolation.

295 **Flow cytometry**

296 Reporter strain STM WT-*plsr*-GFP and STM *ΔluxS-plsr*-GFP were grown in LB
297 media, and samples were taken out at different time points and fixed with 3.5%
298 paraformaldehyde. The positive GFP percentage population was determined in
299 the sample by using BD FACS Verse.

300 ***In vivo* animal experiment**

301 Male C57BL/6, aged 5 to 6 weeks, were obtained from the Central Animal
302 Facility, IISc.

303 **Invasion assay**- 5–6 weeks old C57BL/6 mice were infected by orally gavaging
304 107 CFU of STM WT, STM *ΔluxS*, STM *ΔlsrB*, STM *ΔlsrK*, STM *ΔlsrR,* and
305 STM *ΔluxS:luxS*. For invasion assay intestine was isolated 6 h post-infection, and
306 CFU was enumerated on differential and selective SS agar by serial dilution

307 followed by plating. BF-8 (10 μg/ml) treated STM WT culture and DPD
308 supplementation (100 μM DPD) or STM WT spent media treated STM Δ*luxS* was
309 used for invasion study in mice.

310 ***In vivo*, competition assay-** Competition assay was done between STM WT and
311 STM*ΔluxS*/STM*ΔlsrB*/STM*ΔlsrK*. Infection was given by oral gavaging with 107
312 CFU/ml of culture in a 1:1 ratio. Post five days of infection, the intestine (Peyer's
313 patches), MLN (mesenteric lymph node), spleen, liver, and blood were
314 aseptically extracted to examine the colonization in the organs. The CFU was
315 enumerated on differential and selective *Salmonella-Shigella* (SS) agar and
316 respective antibiotics containing LB agar plates. The competitive index was
317 calculated for a WT strain and knockout strains by dividing the ratio between
318 CFU (Knockout strain) and CFU (STM WT) by the ratio of both strains in the
319 inoculum.

320 ***In vivo* infection and BF-8/antibiotics treatment**- 5–6 weeks old C57BL/6 mice
321 were infected by orally gavaging 10^7 CFU of STM WT. Post 3rd day of infection,
322 one cohort of mice was sacrificed for the organ burden of *Salmonella*. The rest of
323 the cohort of mice were treated with either 2mg/kg of body weight of BF-8,
324 ciprofloxacin, ceftazidime, or a combination of BF-8 with both antibiotics
325 intraperitoneally for three consecutive days. After the 3rd day of treatment, mice
326 were sacrificed the next day, and the organ burden was determined by CFU
327 enumeration.

328 **Mice survival assay**

329 The mice were given 10^7CFU of STM WT (overnight grown cultures) orally to
330 compare the survival and weight alterations of mice post-infection and BF-8
331 /antibiotics treatment. Post 3rd day of infection, mice were treated with either
332 2mg/kg of mouse weight of BF-8, ciprofloxacin, ceftazidime, or a combination
333 of BF-8 with both antibiotics, intraperitoneally for three consecutive days. The
334 mice were observed every day to determine their survival and weight, and the
335 results were expressed as a percentage of survival (Kaplan-meier curve) and
336 weight reduction.

337 All experiments comply with the rules set forth by the Indian Institute of Science,
338 Bangalore's IEAC. The approved protocol number is CAF/ Ethics/852/2021. The
339 Institutional Animal Ethics Committee approved every animal experiment, and
340 the National Animal Care Guidelines were scrupulously followed.

341 **Statistical analysis**

342 As mentioned in figure legends, each experiment has been independently
343 repeated two to five times. GraphPad Prism 8.4.3 was utilized for all statistical
344 analyses. As the figure legends state, the statistical analyses included an unpaired,
345 two-tailed Student's t-test, One-way ANOVA with Dunnet's post hoc test, Two-
346 way ANOVA with Tukey's post hoc test. A non-parametric one-way ANOVA
347 (Kruskal Wallis) test with Dunn's post-hoc test was performed for the animal
348 experiment. P-values less than 0.05 were regarded as significant. The analysis is

349 presented as mean ±SD or mean ±SEM with information on group sizes and p

350 values mentioned in the respective figure legends.

351

352 **Results**

353 **Autoinducer-2 signaling governs bacterial Motility and flagellar**
354 **organization by modulating chemotaxis and flagella-related genes**

355 We first investigated whether *Salmonella* LuxS/AI-2 signaling is involved in
356 Motility. As reported, the aggregation of *E. coli* towards AI-2 depends on Motility
357 and chemotaxis(24),we have also observed that upon deletion of *luxS*, *lsrB*, and
358 *lsrK*, swim and swarm Motility were hampered compared to STM WT **(Fig.1A,**
359 **B; S1A, B)**.

360 Many motile bacteria control their swimming direction by regulating the sense of
361 flagellar rotation in response to sensory cues. FliM is a key component of the
362 flagellar motor's switch complex, along with FliG and FliN, which is thought to
363 interact with one of the chemotaxis proteins, CheY(40, 41). The result of these
364 interactions is to induce clockwise rotation of the flagellar motors and tumbling
365 of the cell. We hypothesized that Lux/AI-2 signaling, due to its virtue of
366 orchestrating gene expression, might regulate the expression of these genes to
367 modulate Motility. We observed that *in vitro* LB media, *fliM*, *cheY,* and *motA*
368 (regarded as the stator of the flagellar motor)(42), mRNA expression was
369 downregulated in STM *ΔluxS*, STM *ΔlsrB*, STM *ΔlsrK* compared to STM WT
370 **(Fig.1C-E)**. Following this, we noted that genes involved in transcription
371 regulation of flagella assembly *flhD, fliA, fliC, fljB*,(43) were also downregulated
372 in the absence of AI-2 accumulation and phosphorylation **(S1 C-F)**. We further
373 observed that in the absence of AI-2 sensing and signaling, the number of flagella

374 is reduced on the surface of STM *ΔluxS* and STM *ΔlsrK*, while there were no
375 flagella on the surface of *STM ΔlsrB*. We further validated with inhibition of AI-
376 2 signaling using BF-8, a competitive inhibitor of DPD in STM WT and
377 supplementing with exogenous DPD and STM WT spent media to STM *ΔluxS.*
378 We observed that BF-8 treatment reduced and DPD or spent media treatment
379 increased the flagella number (Fig.1F). From these data, we concluded that
380 LuxS/AI-2 signaling governs Motility and flagellar organisation via regulating
381 flagella and chemotaxis-related gene expression.

382 **AI-2 sensing in *Salmonella* assists in chemotaxis and enhances the**
383 **attachment to Caco-2 epithelial cells**

384 Studies show that in *E.coli,* AI-2 binds LsrB, and L-serine binds Tsr
385 chemoreceptor, and both LsrB and Tsr are necessary for sensing AI-2, but not for
386 AI-2 uptake. This suggests that LsrB and Tsr interact directly in the periplasm
387 within *E.coli*(27). We speculate that the LsrB receptor in *Salmonella* may act as
388 a chemoreceptor and aid in the attraction to the AI-2 molecule. We used a μ-Slide
389 Chemotaxis chamber (ibidi) for the chemotaxis assay. DPD, STM WT spent
390 media, and serine were used in the second reservoir of the chamber. Serine was
391 used as a positive control as a chemoattractant. We found that the number of STM
392 WT transmigrated towards spent media, DPD, and serine was higher compared
393 to STM *ΔluxS* and STM *ΔlsrB* **(Fig.2 A-C)**. The explanation for the reduced
394 transmigration of STM *ΔluxS* and STM *ΔlsrB* toward serine is due to reduced

395 flagella activity. These data suggest that LuxS/AI-2 signaling controls flagellar
396 Motility and chemotaxis.
397 Replicating laboratory conditions that accurately reflect the natural microbial
398 habitat during infection presents significant challenges. Consequently, fluid flow,
399 a defining characteristic of natural environments, is often ignored in experimental
400 setups. However, with the development of microfluidic technology coupled with
401 high-resolution imaging, it is now possible to understand environmental features
402 that affect bacterial pathogenesis(44). But this natural flow can remove the
403 autoinducer molecule and hamper the signaling. A study revealed that *S. aureus*
404 produces enterotoxin B in crypts, deepening them and insulating the bacteria from
405 flow, facilitating QS-regulated pathogenicity(45). Similarly, *V. cholerae* activates
406 QS within, but not outside, intestinal crevices, highlighting the role of topography
407 in virulence(46, 47). *Salmonella* is a pathogen that primarily infects the ileum,
408 the distal part of the small intestine(48). *Salmonella* has evolved mechanisms to
409 gain access, attach, and infect the intestinal epithelial cells of the crypt to survive
410 and replicate. We speculate that *Salmonella* is attracted towards AI-2 molecules
411 of the intestinal crypts, where fluid flow is resisted, and it can answer why
412 *Salmonella* moves to the distal part of the intestine. Epithelial cells release an AI-
413 2 mimic in response to bacteria, and bacteria might benefit from this AI-2 mimic
414 via their AI-2 quorum-sensing receptors(26). We were curious whether LuxS/AI-
415 2 modulates the attachment to epithelial cells. Our adhesion assay suggests that
416 STM *ΔluxS*, STM *ΔlsrB*, and *ΔlsrK* compromised their ability to adhere to Caco-

417 2 epithelial cells **(Fig. 2D, E, S2A).** On the other hand, STM *ΔlsrR* behaves
418 similarly to STM WT. Upon inhibition of LuxS/AI-2 signaling with BF-8 in STM
419 WT and exogenous DPD and STM WT spent media treatment to STM *ΔluxS,*
420 suggests AI-2 sensing and signaling enhance the attachment to epithelial cells
421 **(Fig. 2F).**

422 ***Salmonella* exploits its LuxS/AI-2 mediated communication to invade**
423 **intestinal epithelial cells**

424 Adhesion and invasion represent the crucial step of successfully establishing
425 infection by bacterial pathogens and cellular invasion, which is followed by
426 intracellular multiplication, dissemination to other tissues, or persistence(39, 49,
427 50). Having observed that LuxS/AI-2 enhances the attachment to Caco-2 cells,
428 we also conjecture that LuxS/AI-2 signaling regulates the invasion of *Salmonella*
429 into the epithelial cells. We infected the Caco-2 epithelial cell with STM stains
430 and observed that STM WT, *luxS* complemented in STM *ΔluxS,* and STM *ΔlsrR*
431 invade more efficiently compared to STM *ΔluxS*, STM *ΔlsrB*, and *ΔlsrK* **(Fig.**
432 **3A)**. Further, we treated the STM *ΔluxS* with exogenous DPD and STM WT spent
433 media and STM WT with inhibitor BF-8 followed by infection in Caco-2
434 epithelial cells. Exogenous DPD and spent media treatment recovered the
435 invasion compared to untreated STM *ΔluxS,* while upon inhibition with BF-8, the
436 STM WT invasion was reduced **(S3 A-C)**. Next, to validate our *in vitro* cell line
437 results, we then studied the invasion of the knockout strains into the intestine of
438 C57BL/6 mice **(Fig. 3B).** Interestingly, STM *ΔluxS*, STM *ΔlsrB*, and *ΔlsrK*

439 invaded significantly less into the Peyer's patches of the C57BL/6 mice **(Fig. 3C)**.
440 STM WT invasion was reduced upon BF-8 treatment. In contrast, STM *ΔluxS*
441 invasion increased with the treatment of DPD and STM WT spent media **(S4A)**.
442 The immunofluorescence study with the histopathological sections of the mouse
443 ileum further validated the reduced invasion and colonization of the mutants in
444 the intestine **(Fig. 3D; S4B)**.
445 It is shown that the master regulator HilD regulates *Salmonella* invasion and
446 Motility via activating gene expression of the type 3 secretion system 1 (SPI-1)
447 and motility genes(51, 52). We hypothesized that LuxS/AI-2 signaling regulates
448 the *hilD* and other SPI-1 master regulators to modulate the invasion or infection
449 in host cells. We observed that *hilD, hilA,* and *invF* master regulators of SPI-1
450 were downregulated in STM *ΔluxS*, STM *ΔlsrB*, and STM *ΔlsrK in vitro* LB
451 media compared to STM WT **(Fig. 4 E-G)**. Thus, *Salmonella* requires LuxS/AI-
452 2 signaling to invade successfully within the IECs *in vitro* and *in vivo* via
453 regulating SPI-1 regulators.
454 **LuxS/AI-2 signaling is active and facilitates survival within Caco-2 epithelial**
455 **cells**
456 As the LuxS/AI-2 signaling is a key language for *Salmonella* communication, ,
457 we sought to explore its role in the next stages of infection. To begin, we asked
458 how *Salmonella* Typhimurium regulates the expression of the genes within the
459 *lsr* operon and *luxS* upon infection into host cells? We evaluated the mRNA
460 expression of *luxS* and *lsr* operon genes (*lsrB*, *lsrK*, *lsrR*) in STM WT upon

461 infection in the Caco2 cell line. We noted that the *lsr* operon genes were slightly
462 higher at post 6h infection compared to 2h post-infection, and further, it
463 downregulated at late 16h post-infection **(Fig. 4A)** while *luxS* expression was
464 similar at 2h and 6h post-infection and downregulated at 16h post-infection
465 compared to 2h **(Fig. 4B)**. Consistent expression of genes suggests that AI-2
466 signaling may be active inside the host cell. Following this, we observed that
467 STM *ΔluxS*, STM *ΔlsrB*, and STM *ΔlsrK* proliferate less in comparison to STM
468 WT, STM *ΔlsrR,* and *luxS* complemented STM *ΔluxS* within the Caco-2 cells
469 **(Fig. 4C)**. The fold replication was reduced in the BF-8-treated culture of STM
470 WT **(Fig. 4D)**. Conversely, upon treatment of WT spent media and exogenous
471 DPD molecule, STM *ΔluxS* fold replication was recovered **(S5A, B)**. To further
472 confirm whether this signaling is active inside the host cells, we generated the
473 reporter strain, which produces green fluorescence on LuxS/AI-2 activation.
474 Firstly, we checked the quorum sensing active bacteria during the *in vitro* growth
475 in LB media. Flow cytometry and fluorescence microscopy results suggest that
476 quorum-sensing active bacterial cells were increased in mid-log phase to early
477 stationary phase **(Fig. 4E; S5C)**. Moreover, when we gave the STM WT spent
478 media treatment to STM *ΔluxS* (Containing reporter construct), we observed that
479 STM *ΔluxS* became quorum sensing active (**S5D)**. Upon infection in Caco-2
480 epithelial cells with reporter STM strain suggests that Lux/AI-2 signaling is active
481 inside the host cells **(Fig. 4F)**. Taken together, this suggests that LuxS/AI-2
482 signaling is active and facilitates survival within Caco-2 epithelial cells.

483 **LuxS/AI-2 cascade facilitates *Salmonella* survival by evading host**
484 **antimicrobial peptide defence mechanisms**

485 The innate immune system within the gut relies substatially on antimicrobial
486 peptides (AMPs) from epithelial cells, including cathelicidins and defensins.
487 They help maintain intestinal homeostasis by targeting pathogens and regulating
488 the gut microbiota(53). Our previous study showed that the LsrR repressor
489 protein negatively modulates the expression of the *phoP* gene, which protects
490 against acidic stress(54). Several studies revealed cationic antimicrobial peptides
491 can activate the PhoP/PhoQ two-component system (TCS), and the PhoP/PhoQ
492 two-component system TCS regulates the expression and activation of *pmrABD*
493 and provides protection against the AMPs (55-62). We considered that LuxS/AI-
494 2 signaling might aid in combating antimicrobial peptide sensitivity via
495 regulating *phoP/phoQ*. In continuation, we observed that STM *ΔluxS*, STM
496 *ΔlsrB*, and STM *ΔlsrK* were more sensitive compared to STM WT and STM
497 *ΔlsrR* under *in vitro* conditions in the presence of sub-MIC concentration of
498 polymyxin **(Fig. 5A; S 6A, B)**. Subsequently, we found that the mRNA
499 expression levels of *pmrD*, *pmrA*, and *pmrB* were reduced in STM *ΔluxS*, STM
500 *ΔlsrB*, and STM *ΔlsrK* compared to STM WT under polymyxin-treated
501 conditions *in vitro* in LB media **(Fig. 5B)**. However, in STM *ΔlsrR*, their
502 expression levels were comparable to those in STM WT. Thereafter, *pmrD*, *pmrA*,
503 and *pmrB* gene expression level reduction was observed upon infection in Caco-
504 2 epithelial cells in STM *ΔluxS*, STM *ΔlsrB*, and STM *ΔlsrK* compared to STM

505 WT **(Fig. 5 C-E)**. Conclusively, LuxS/AI-2 signaling facilitates survival within
506 Caco-2 epithelial cells by regulating the *pmrD/AB* gene expression.

507 **LuxS/AI-2 signaling regulates critical gene targets to assist in multiple stages**
508 **of *Salmonella* infection in the host**

509 As we observed, LuxS/AI-2 signaling is involved in various stages of *Salmonella*
510 infection by regulating multiple genes. Following this, we performed
511 transcriptomic analysis between STM WT and quorum sensing knockout strains
512 STM *ΔluxS*, STM *ΔlsrB, and* STM *ΔlsrK.* We figured out that over the 4728 gene
513 variables, 507, 1291, and 225 genes were significantly differentially expressed in
514 STM *ΔluxS*, STM *ΔlsrB,* and STM *ΔlsrK,* respectively. Out of which, 316 are
515 down-regulated and 191 are up-regulated in STM *ΔluxS,* 902 are down-regulated
516 and 389 genes are up-regulated in STM *ΔlsrB,* while 106 are down-regulated and
517 119 are up-regulated in STM *ΔlsrK* in comparison to STM WT **(Fig. 6A-C)**. Gene
518 enrichment and KEGG analysis revealed that down-regulated genes belong to the
519 flagellar classes (*fliC*/*fljB* family gene), chemotaxis (*cheY*, *motA*, *motB* etc.),
520 secretory protein and virulence-associated genes (*sopD2*, *sseI*, *pipB*, *sopB*, *sifA*)
521 etc **(Fig. 6D, E)**. Interestingly, the heatmap of the top 50 genes also includes genes
522 related to flagellar motility *fliC*/*fljB*, chemotaxis gene *motA,* and virulence genes
523 (*hilD*, *pipB*, *sseI,* etc.) **(S7A-C)**. Taken together, the transcriptomic analysis
524 suggests that the Lux/AI-2 signaling regulates multiple critical gene targets to
525 assist in multiple stages of *Salmonella* infection in the host.

526 **Inhibition of LuxS/AI-2 signaling with antibiotics reduces *Salmonella***
527 **colonization *in vivo* and enhances mice survival**
528 *Salmonella* can mediate its uptake into enterocytes by delivering effector
529 molecules through Type 3 secretion systems (T3SS). It can also be phagocytosed
530 by immune cells such as macrophages, dendritic cells, and neutrophils residing
531 in Peyer's patches. However, *Salmonella* preferentially enters specialized cells
532 called microfold cells or M-cells of the Peyer's patches in the intestinal
533 epithelium. After breaching the epithelial cells at the Peyer's patches in the distal
534 ileum, it disseminates to the liver, spleen, and mesenteric lymph node (MLN), the
535 secondary infection sites(63, 64). *Salmonella* is known to be a successful
536 pathogen that can overcome various host immune responses such as oxidative
537 stress, nitrosative stress, acidic pH, etc(65). In our recent study, STM *ΔluxS*, STM
538 *ΔlsrB*, and STM *ΔlsrK* showed less colonization and delayed mouse mortality
539 compared to STM WT infection, and upon treatment of BF-8 (4mg/kg mice body
540 weight) to STM WT-infected mice, organ burden was reduced, and mouse
541 survivability increased(54). Following this, we observed in competition between
542 STM WT with STM *ΔluxS* or STM *ΔlsrB*, or STM *ΔlsrK* in mice co-infection
543 studies, STM WT outcompeted all three mutants in the liver, spleen, MLN, and
544 intestine **(Fig. 7A, B)**. Further, we questioned whether, upon treatment with BF-
545 8 in combination with low-concentration doses (2mg/kg of each) of antibiotics
546 ciprofloxacin and ceftazidime, the infection and mortality of mice could be cured.
547 So, we first infected the mice with STM WT by oral gavage and started the

548 treatment on the 3rd day post-infection (Fig. 7C). On the 3rd day post-infection,
549 we observed organ colonization and slight weight reduction, confirming infection
550 **(S8 A-C)**. After each day of treatment of BF-8 with or without antibiotics for
551 consecutive days, on the 6th day post-infection, we noted that organ colonization
552 was significantly less with the combination of low concentration 2mg/kg of body
553 weight (of BF-8 and ciprofloxacin or ceftazidime **(Fig. 7C-F; S8D, E)**. With the
554 treatment of three doses of a combination of BF-8 with ciprofloxacin or
555 ceftazidime, started on the 3rd day post-infection, mice survived till 14 or 15 days,
556 respectively. On the other hand, low doses of BF-8 and antibiotics also delayed
557 the mortality of mice compared to the untreated mice **(Fig. 7G, H; S8 F)**.
558 Furthermore, tissue histopathology of liver and spleen, suggested that a
559 combination treatment of BF-8 inhibitor with antibiotics improved the health of
560 the mice more effectively with a less disease score (**Fig. 7I; S9)**. These data
561 suggest that the AI-2 mediated signaling is required for *in vivo* colonization of
562 *Salmonella* in mice, and signaling inhibition can be a promising strategy in
563 combination with low doses of antibiotics for treatment of *Salmonella* infection
564 in the era of emerging antibiotic-resistant *Salmonella* strains.
565

566 **Discussion**

567 Adapting its tactics and employing multiple defense systems, *Salmonella* has
568 become a potent enteric pathogen, occupying several host niches during its
569 pathogenesis. The opening moves during its pathogenesis involve the expansion
570 and competition in the gut, followed by attachment and invasion. To do so,
571 *Salmonella* must first reach the site of infection. Of the several factors,
572 chemotaxis and Motility contribute majorly to such a process. Recently, it was
573 shown that AI-2, a quorum-sensing molecule, can work as a chemoattractant and
574 help in aggregation(24). Here, we showed that *Salmonella* LuxS/AI-2 signaling
575 controls Motility via regulating Motility, flagellar gene expression, and flagellar
576 organisation. *Salmonella* produces and releases the AI-2 molecules, which, upon
577 reaching an optimal concentration in the environment, begin to accumulate
578 intracellularly via the ABC transporter. The phosphorylation of the intracellular
579 AI-2 by LsrK is crucial for its function and orchestration of its gene targets (66).
580 Since the accumulation of AI-2 upregulates the *lsr* operon, we also observe that
581 the genes *lsrB*, *lsrK*, and *lsrR* were upregulated during the mid-log and late-log
582 phases(54). This provides an additional context to our current observations, as
583 flagella formation is primarily during its exponential growth phases *in vitro*.

584 The gastrointestinal tract is a dynamic environment where microbes compete for
585 space and nutrients through various mechanisms. Many gut-associated bacteria
586 produce AI-2 via the LuxS enzyme, including a significant proportion of
587 Firmicutes and Proteobacteria, and a few members of the phyla Bacteroidetes and

588 Actinobacteria. (67, 68). Besides, species of the families Barnesiellaceae and
589 Muribaculaceae also contribute to AI-2 production in the gut (69). Being an
590 enteric pathogen and a sensor of the universal communication signal, *Salmonella*
591 may profit from the AI-2 produced by the gut commensal in the intestinal lumen.
592 Through its ABC transporter, *Salmonella* may readily take up the extracellular
593 AI-2 produced by the gut microbes. This further demonstrates that intra-bacterial
594 communication and interactions might be exploited by pathogens to win the arms
595 race.
596 Natural fluid flow in the intestine can remove autoinducers, disrupting quorum
597 sensing. *Staphylococcus aureus* utilizes autoinducers in the crypts (non-existent
598 flow) and enhances pathogenicity by producing enterotoxin B (45). Similarly,
599 *Salmonella* targets the ileum crypts to invade epithelial cells, ensuring survival
600 and replication. Natural dynamics are crucial in bacterial adaptation and
601 virulence(48). Motility towards the ileum of the intestine is essential, and sensing
602 AI-2 plays a pivotal role in *Salmonella* pathogenesis. Our results suggest that
603 *Salmonella* can move toward the AI-2 molecule, and LsrB might work as a
604 chemoreceptor. As previously studied, LsrB in *E.coli* acts as a receptor for AI-2
605 and aids in the sensing and drives chemotaxis towards the AI-2 pool (70).
606 Similarly, we speculate that in *Salmonella,* the LsrB receptor also assists in
607 sensing AI-2, while the AI-2 is internalised through the ABC receptor, which
608 tunes the expression of chemotaxis and motility gene expression to drive motion
609 towards the AI-2 pool. HilD is the master regulator of Motility and the SPI-1

610 gene. The present study shows that LuxS/AI-2 signaling regulates the *hilD* gene
611 expression, thereby aiding in Motility, attachment, and invasion of epithelial cells
612 *in vitro* and *in vivo* conditions. Additionally, we observe that the SPI-1 genes *hilA*
613 and *invF* are also underexpressed in the quorum-sensing mutants. This likely
614 accounts for the impaired adhesion and invasion of these mutants, as the SPI-1
615 encoded T3SS system and effector molecule mediate host cell invasion.
616 Our findings further indicated that accumulation and phosphorylation of AI-2 are
617 necessary for controlling the expression of the *pmrD/AB*. The *pmrD/AB* could be
618 regulated by PhoP, resulting in reduced survival of STM *ΔluxS*, STM *ΔlsrB*, and
619 STM *ΔlsrK in vitro* and in the epithelial cells (71, 72). Our previous study
620 highlighted the regulatory mechanism of LuxS/AI-2 in controlling the *phoP/Q*
621 transcription (54). Hence, in such a context, our present study further highlights
622 the broader, interconnected regulatory roles of LuxS/AI-2 in several defence
623 strategies of this pathogen. Transcriptomic analysis revealed that LuxS/AI-2, the
624 language of *Salmonella,* can control various critical genes in *Salmonella.* These
625 genes are involved in flagellar motility, invasion, cell surface and membrane
626 functions, and secretory pathways. This underscores how the quorum-sensing
627 cascade regulates numerous genetic programs that are involved in the various
628 stages of *Salmonella* infection. As previously reported, the regulation of the
629 *phoP/Q* operon by the LsrR repressor through the promoter binding activity of
630 the repressor, it can be assumed that some of these genetic controls may also
631 involve the LsrR binding activity (54). Our present work also demonstrated that

632 the organ burden of *Salmonella* was reduced upon treatment of mice with
633 inhibitor BF-8 in combination with low doses of antibiotics ciprofloxacin and
634 ceftazidime. Considering the increasing emergence of antimicrobial-resistant
635 *Salmonella* strains worldwide, there is a need for alternative approaches to curb
636 infection. As we point out to the broader and interconnected regulatory
637 mechanisms by the LuxS/AI-2 signaling in *Salmonella*, intervening in such a
638 critical signaling process proves to be a promising infection resolution strategy.
639 Considering the pervasive presence of AI-2, it appears paradoxical that
640 *Salmonella* cells depend on it to colonize a specific niche within the gut. One
641 plausible rationale for this might be that AI-2 chemotaxis becomes significant
642 under dysbiosis conditions that suppress microbiota and promote the proliferation
643 of *Enterobacteriaceae* (73, 74). Our study provides evidence for a causal link
644 between AI-2 chemotaxis, gut colonization, and niche segregation of *Salmonella*
645 strains in the murine gut. It further establishes a link between AI-2 chemotaxis,
646 invasion, and colonization *in vivo*. We suggest that similar mechanisms of AI-2-
647 mediated host colonization might exist in other chemotactic enteric bacteria, and
648 inhibition of LuxS/AI-2 signaling might open avenues for antibiotic resistance of
649 pathogenic bacteria.

Funding

This work was funded by the Department of Biotechnology (DBT), Ministry of Science and Technology, the Department of Science and Technology (DST), Ministry of Science and Technology. DC acknowledges DAE-SRC (DAE00195) outstanding investigator award and funds and ASTRA Chair Professorship funds. The authors jointly acknowledge the DBT-IISc partnership program. Infrastructure support from ICMR (Center for Advanced Study in Molecular Medicine), DST (FIST), UGC-CAS (special assistance), and TATA fellowship is acknowledged. AS duly acknowledges UGC-SRF for the financial assistance. AVN duly acknowledges the IISc-MHRD for the financial assistance.

Ethics statement

All experiments comply with the rules set forth by the Indian Institute of Science, Bangalore's IEAC. The approved protocol number is CAF/ Ethics/852/2021. The Committee for Control and Supervision of Experiments on Animals (CPCSEA), a statutory committee established under Chapter 4, Section 15 (1) of the Prevention of Cruelty to Animals Act 1960, and National Animal Care provided guidelines that were meticulously adhered to during all animal experiments, all of which were approved by the Institutional Animal Ethics Committee. (Registration No. 435 48/1999/ CPCSEA). The Institutional Animal Ethics Committee approved every animal experiment, and the National Animal Care Guidelines were meticulously followed.

Author contribution

AS and DC conceived the study. AS and DC designed experiments. AS performed experiments. AS and AVN performed an electron microscopy experiment. RSR analyzed the tissue histopathology. AS analyzed the data, prepared the figures, and drafted the manuscript. AS, AVN, and DC reviewed and edited the manuscript. DC supervised the work. All the authors read and approved the manuscript.

Declaration of competing interest

The authors declare no conflict of interest.

Acknowledgment

The Departmental and Divisional Confocal Facility, Departmental Real-Time PCR Facility, Divisional Electron Microscopy facility, and Central Animal Facility at IISc are duly acknowledged. Mr. Arjun and Ms. Syama are acknowledged for their help with image acquisition. Ms. Kirtan is acknowledged for her help with Electron microscope image acquisition. Ms. Aneesha and Ms. Nanditha are acknowledged for their technical help.

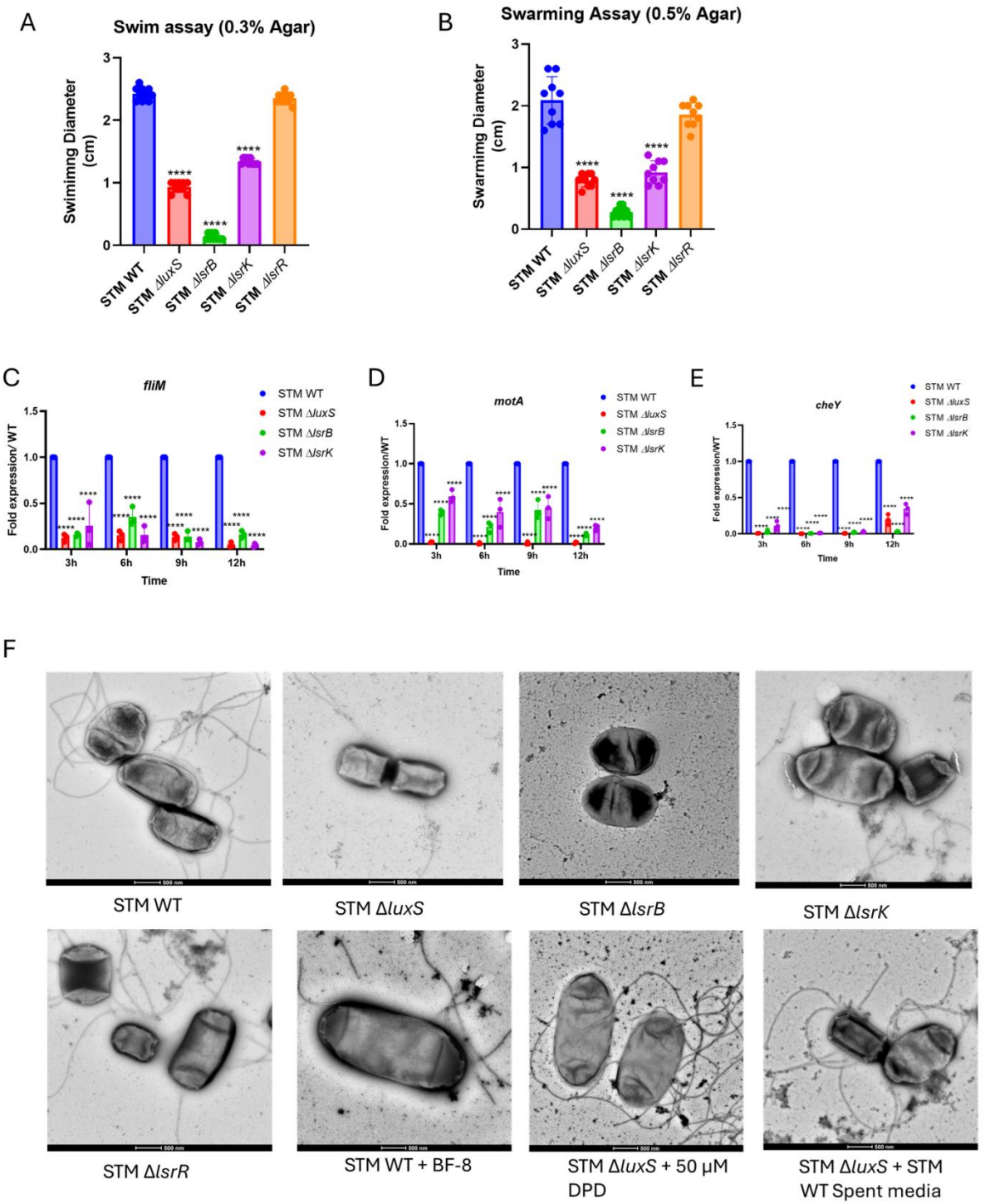

Fig.1 Autoinducer-2 signaling governs bacterial Motility and flagellar organization by modulating chemotaxis and flagella-related genes. (A) Swim Motility, **(B)** Swarm motility assay. Measurement has been taken at three angles per plate. Represented as Mean+/-SD of N=3, n=3. **(C)** mRNA expression of

693 *fliM*, *motA,* and *cheY* STM strains *in vitro* growth in LB. Represented as Mean+/-
694 SD of N=3, n=3, **(D)** Transmission electron microscope representative image of
695 STM strains. Represented as Mean+/-SD of N=2, n>10. One-way ANOVA with
696 Dunnet's post-hoc test was used to analyze the data; p values **** $p < 0.0001$,
697 *** $p < 0.001$, ** $p<0.01$, * $p<0.05$. Two-way Anova was used to analyze the
698 grouped data; p values **** $p < 0.0001$, *** $p < 0.001$, ** $p<0.01$, * $p<0.05$

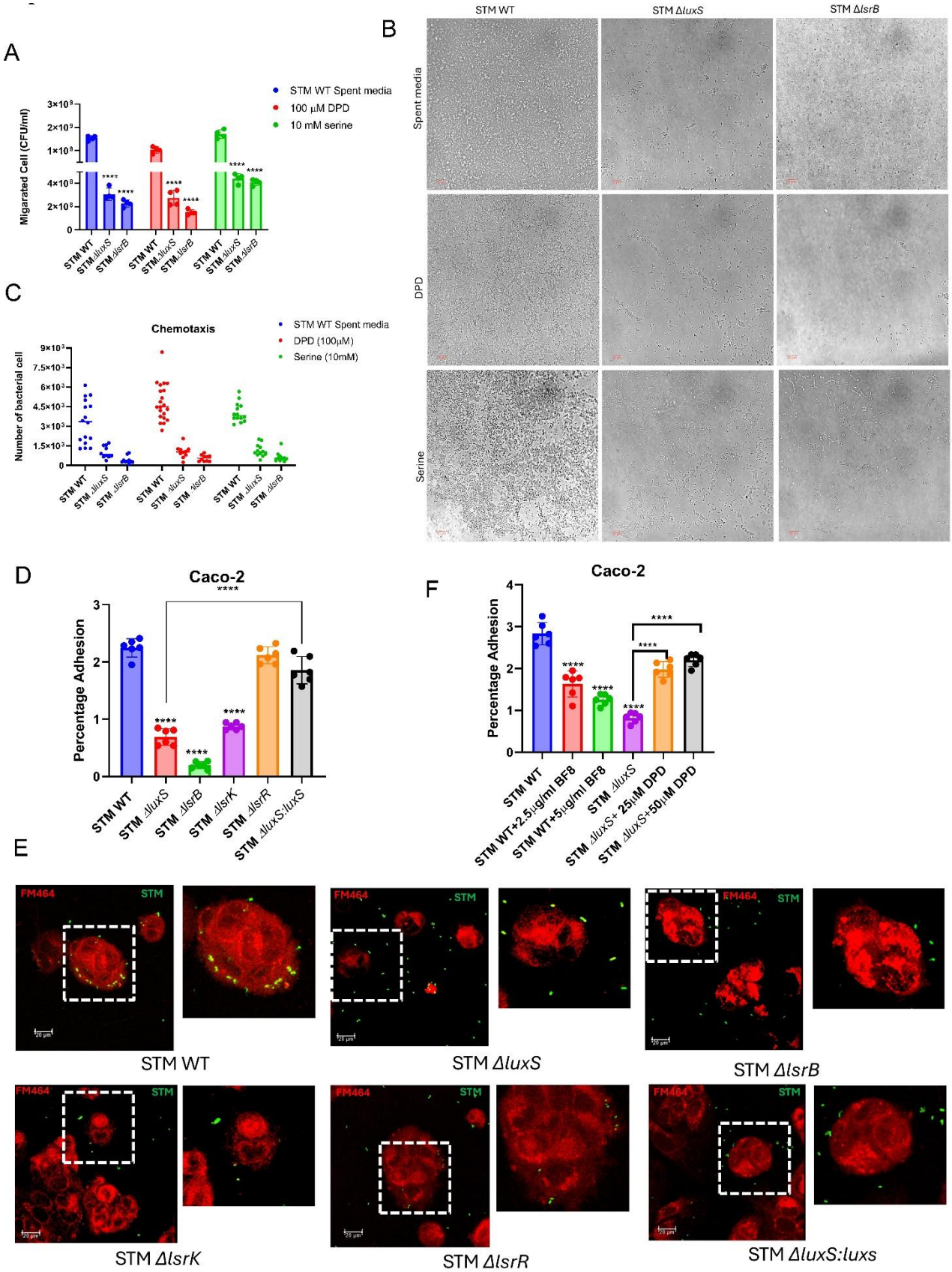
A
Migarated Cell (CFU/ml)
STM WT Spent media
100 μM DPD
10 mM serine
STM WT
STM ΔluxS
STM ΔlsrB
B
STM WT
STM ΔluxS
STM ΔlsrB
Spent media
DPD
Serine
C
Chemotaxis
Number of bacterial cell
STM WT Spent media
DPD (100μM)
Serine (10mM)
D
Caco-2
Percentage Adhesion
STM WT
STM ΔluxS
STM ΔlsrB
STM ΔlsrK
STM ΔlsrR
STM ΔluxS:luxS
F
Caco-2
Percentage Adhesion
STM WT
STM WT+2.5μg/ml BF8
STM WT+5μg/ml BF8
STM ΔluxS
STM ΔluxS+ 25μM DPD
STM ΔluxS+50μM DPD
E
FM464
STM
STM WT
STM ΔluxS
STM ΔlsrB
STM ΔlsrK
STM ΔlsrR
STM ΔluxS:luxs

699

700 **Fig. 2 AI-2 sensing in *Salmonella* assists in chemotaxis and enhances the**
701 **attachment to Caco-2 epithelial cells. (A)** CFU analysis of transmigrated STM
702 strains towards STM WT spent media, DPD, and known chemoattractant serine.
703 The experiment was performed in an ibidi chemotaxis chamber. Represented as
704 Mean+/-SD of N=3, n=2. **(B)** Bright-field microscopy images of transmigrated
705 bacteria. **(C)** Analysis of images using ImageJ software to count the number of
706 bacteria per image. Each dot represents per image. The image is represented as
707 Mean+/-SD of N=3, n>10. **(D)** Adhesion assay of STM WT, STM *ΔluxS*, STM
708 *ΔlsrB*, STM *ΔlsrK,* STM *ΔlsrR,* and STM *ΔluxS:luxS* in Caco-2 epithelial cells.
709 Represented as Mean+/-SD of N=3, n=3. **(E)** Immunofluorescence imaging to
710 study the adhesion to Caco-2 cells of STM WT and knockout strains, here
711 FM464(red) is used to stain the lipids for Caco-2, and Anti-*Salmonella* (LPS)
712 (Alexafluor-488 tagged secondary antibody used-Green) for STM.
713 Representative image of N=3, n>10. **(F)** Adhesion assay of STM WT and STM
714 *ΔluxS* treated with BF-8 and DPD, respectively. Represented as Mean+/-SD of
715 N=3, n=3. Two-way Anova was used to analyze the grouped data; p values ****
716 $p < 0.0001$, *** $p < 0.001$, ** $p<0.01$, * $p<0.05$.
717

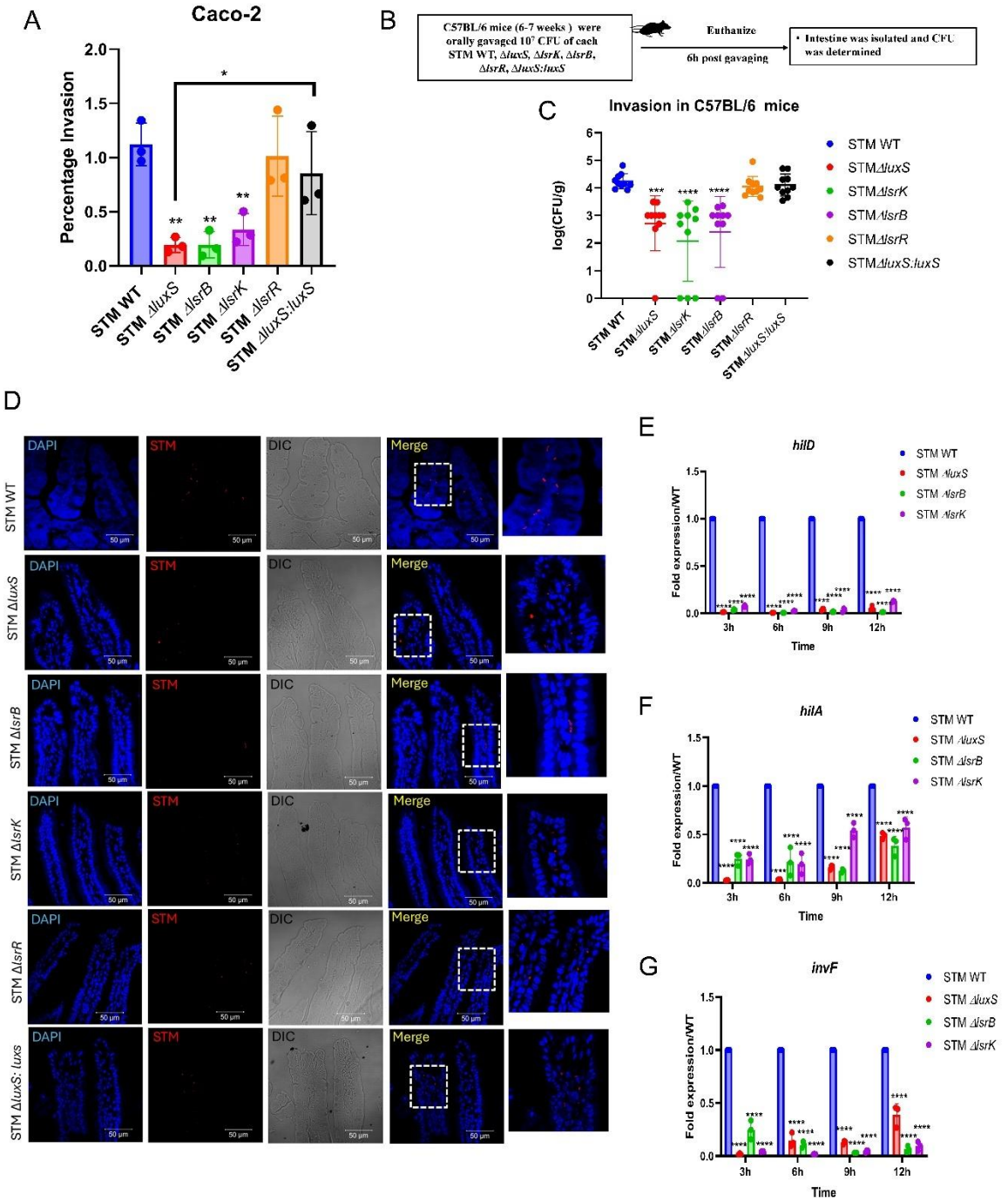

Fig. 3 *Salmonella* exploits its LuxS/AI-2 mediated communication to invade intestinal epithelial cells. (A) Percentage invasion of STM WT, STM *ΔluxS*, STM *ΔlsrB*, STM *ΔlsrK,* STM *ΔlsrR,* and STM *ΔluxS:luxS* in Caco-2 epithelial cells. Represented as Mean+/-SEM of N=3, n=3. **(B)**Experimental schematic representation of the invasion assay in C57BL/6 male mice. **(C)** STM WT, STM

724 *ΔluxS,* STM *ΔlsrB*, STM *ΔlsrK,* STM *ΔlsrR,* and STM *ΔluxS:luxS* invasion assay
725 in mice; organ burden in the intestine post 6h of infection. N=2, n=5.**(D)**
726 Immunofluorescence of histopathological sections of mice intestine (Peyer's
727 patches) to study invasion, DAPI is used to stain the nucleic acids in the cells,
728 and Anti-*Salmonella* (LPS) (Cy3 tagged secondary antibody used-Red). mRNA
729 expression of **(E)** *hilD,* **(F)** *hilA*, **(G)** *invF,* in STM WT, STM *ΔluxS,* STM *ΔlsrB*,
730 and STM *ΔlsrK in vitro* LB media. Represented as Mean+/-SD of N=3, n=3.
731 Represented as Mean+/-SD of N=2, n>10. One-way ANOVA with Dunnet's post-
732 hoc test was used to analyze the data; p values **** $p < 0.0001$, *** $p < 0.001$,
733 ** $p<0.01$, * $p<0.05$. Non-parametric One-way ANOVA (Kruskal Wallis) with
734 Dunn's posthoc test was used to analyze organ burden in mice.Two-way Anova
735 was used to analyze the grouped data; p values **** $p < 0.0001$, *** $p < 0.001$,
736 ** $p<0.01$, * $p<0.05$

737

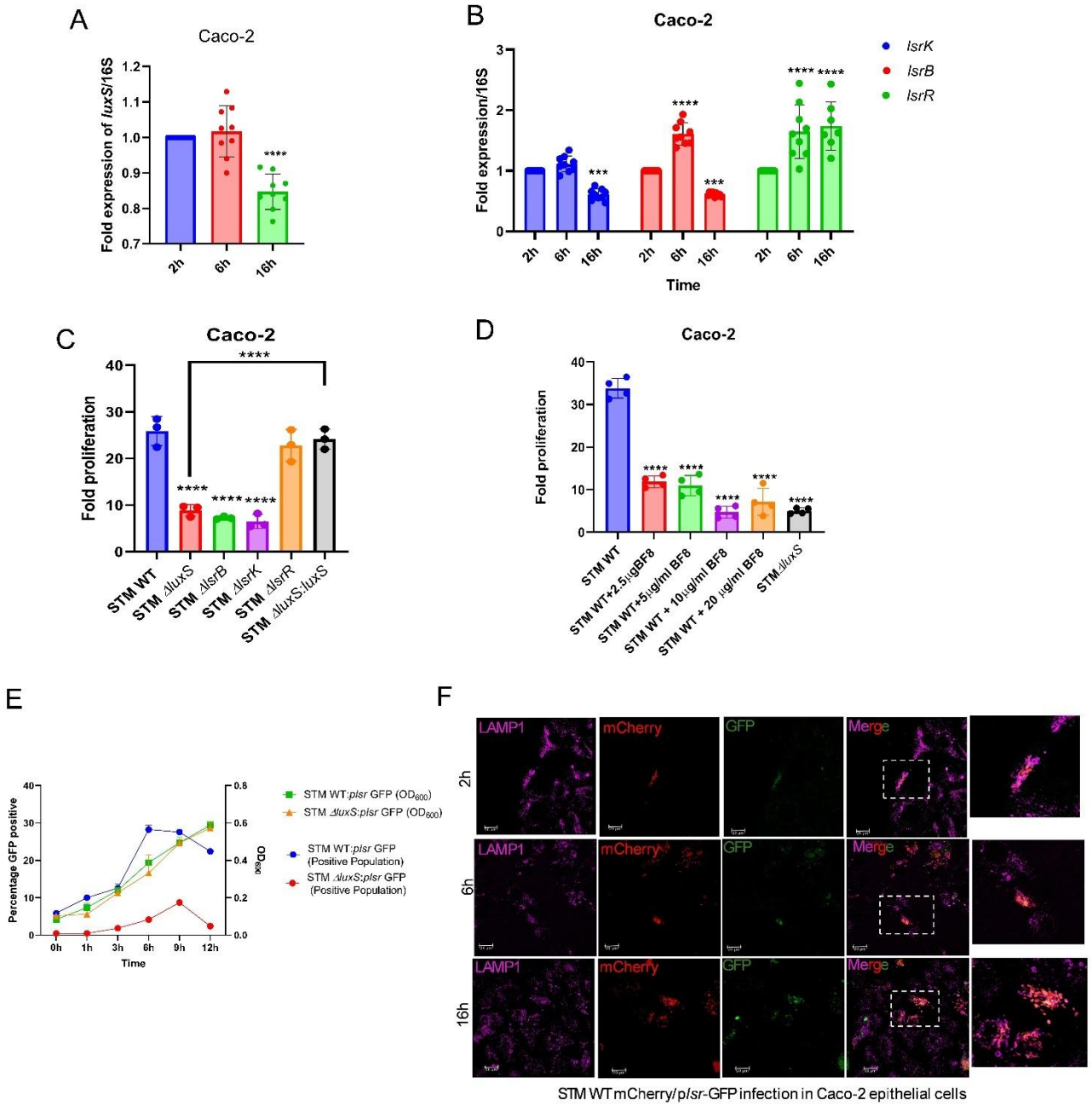

Fig. 4 LuxS/AI-2 signaling is active and facilitates survival within Caco-2 epithelial cells. mRNA expression of **(A)** *luxS,* and **(B)** *lsr* operon genes *lsrB*, *lsrK,* and *lsrR* in STM WT upon infection in Caco-2 epithelial cells. Represented as Mean+/-SDof N=3, n=3. Fold proliferation of **(C)** STM WT and knockout strains, **(D)** STM WT treated with BF-8. Represented as Mean+/-SEM of N=3,

n=3. **(E)** Quorum sensing reporter strains growth kinetics and flow cytometry analysis of GFP-positive bacterial cells. **(F)** Immunofluorescence microscopy analysis of STM WT quorum sensing reporter strains upon infection in Caco-2 epithelial cells. LAMP1 marker- *Salmonella* containing vacuole (SCV), mCherry- Constitutive expression, GFP- quorum sensing active STM. One-way ANOVA with Dunnet's post-hoc test was used to analyze the data; p values **** $p < 0.0001$, *** $p < 0.001$, ** $p<0.01$, * $p<0.05$. Two-way Anova was used to analyze the grouped data; p values **** $p < 0.0001$, *** $p < 0.001$, ** $p<0.01$, * $p<0.05$.

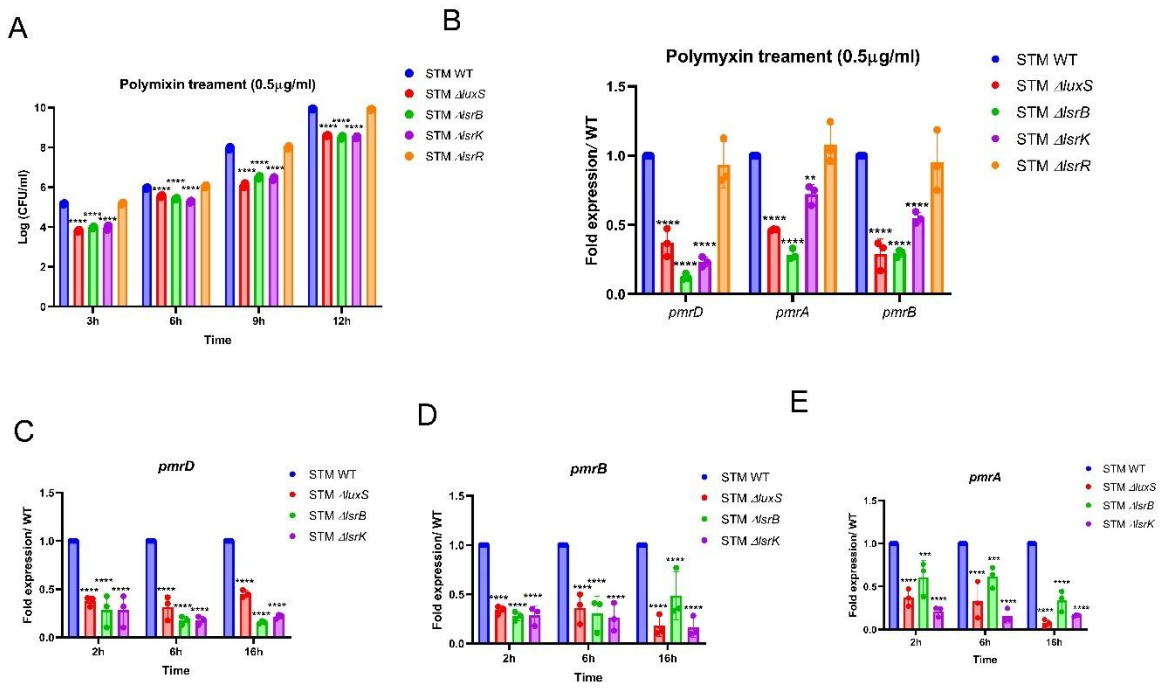

Fig. 5 LuxS/AI-2 cascade facilitates *Salmonella* survival by evading host antimicrobial peptide defence mechanisms. **(A)** *In vitro* polymyxin treatment survival assay of STM WT, STM *ΔluxS*, STM *ΔlsrB*, STM *ΔlsrK,* and STM *ΔlsrR*. Represented as Mean+/-SD of N=3, n=2. **(B)** mRNA expression of *pmrD*, *pmrA,* and *pmrB* in STM WT, STM *ΔluxS*, STM *ΔlsrB*, STM *ΔlsrK,* and STM *ΔlsrR* upon treatment of polymyxin in vitro LB media in mid-log phase culture (6h). Represented as Mean+/-SD of N=3, n=3. mRNA expression of **(C)** *pmrD*, **(D)** *pmrA* and **(E)** *pmrB* in STM WT, STM *ΔluxS*, STM *ΔlsrB*, STM *ΔlsrK,* and STM *ΔlsrR* upon infection in Caco-2 epithelial cells. Represented as Mean+/-SD of N=3, n=3. Two-way Anova was used to analyze the grouped data; p values **** $p < 0.0001$, *** $p < 0.001$, ** $p<0.01$, * $p<0.05$

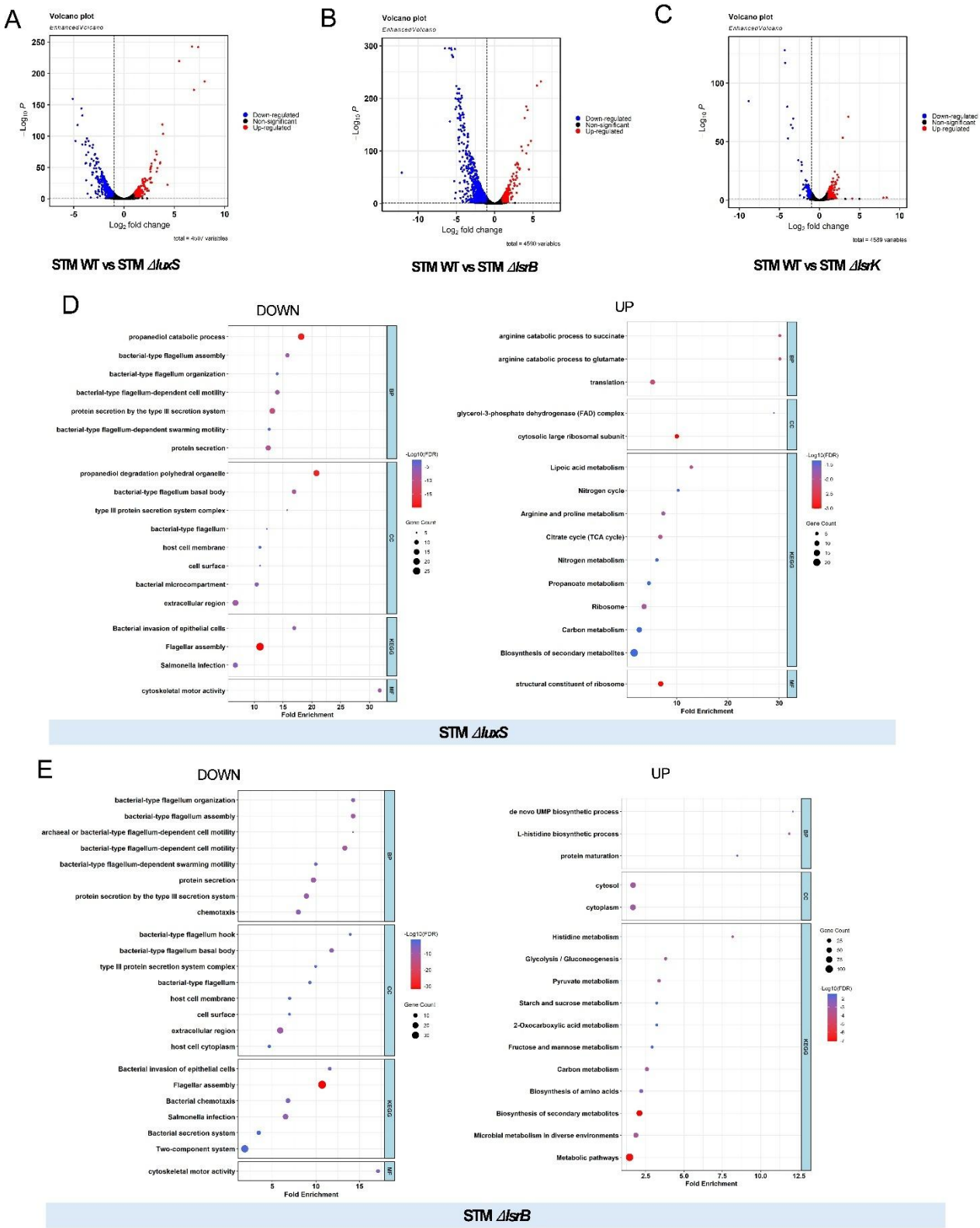
A
Volcano plot
EnhancedVolcano
Log10 P
Log2 fold change
Down-regulated
Non-significant
Up-regulated
STM WT vs STM ΔluxS
B
Volcano plot
EnhancedVolcano
Log10 P
Log2 fold change
Down-regulated
Non-significant
Up-regulated
STM WT vs STM ΔlsrB
C
Volcano plot
EnhancedVolcano
Log10 P
Log2 fold change
Down-regulated
Non-significant
Up-regulated
STM WT vs STM ΔlsrK
D
DOWN
propanediol catabolic process
bacterial-type flagellum assembly
bacterial-type flagellum organization
bacterial-type flagellum-dependent cell motility
protein secretion by the type III secretion system
bacterial-type flagellum-dependent swarming motility
protein secretion
propanediol degradation polyhedral organelle
bacterial-type flagellum basal body
type III protein secretion system complex
bacterial-type flagellum
host cell membrane
cell surface
bacterial microcompartment
extracellular region
Bacterial invasion of epithelial cells
Flagellar assembly
Salmonella infection
cytoskeletal motor activity
BP
CC
KEGG
MF
Fold Enrichment
UP
arginine catabolic process to succinate
arginine catabolic process to glutamate
translation
glycerol-3-phosphate dehydrogenase (FAD) complex
cytosolic large ribosomal subunit
Lipoic acid metabolism
Nitrogen cycle
Arginine and proline metabolism
Citrate cycle (TCA cycle)
Nitrogen metabolism
Propanoate metabolism
Ribosome
Carbon metabolism
Biosynthesis of secondary metabolites
structural constituent of ribosome
Fold Enrichment
STM ΔluxS
E
DOWN
bacterial-type flagellum organization
bacterial-type flagellum assembly
archaeal or bacterial-type flagellum-dependent cell motility
bacterial-type flagellum-dependent cell motility
bacterial-type flagellum-dependent swarming motility
protein secretion
protein secretion by the type III secretion system
chemotaxis
bacterial-type flagellum hook
bacterial-type flagellum basal body
type III protein secretion system complex
bacterial-type flagellum
host cell membrane
cell surface
extracellular region
host cell cytoplasm
Bacterial invasion of epithelial cells
Flagellar assembly
Bacterial chemotaxis
Salmonella infection
Bacterial secretion system
Two-component system
cytoskeletal motor activity
BP
CC
KEGG
MF
Fold Enrichment
UP
de novo UMP biosynthetic process
L-histidine biosynthetic process
protein maturation
cytosol
cytoplasm
Histidine metabolism
Glycolysis / Gluconeogenesis
Pyruvate metabolism
Starch and sucrose metabolism
2-Oxocarboxylic acid metabolism
Fructose and mannose metabolism
Carbon metabolism
Biosynthesis of amino acids
Biosynthesis of secondary metabolites
Microbial metabolism in diverse environments
Metabolic pathways
Fold Enrichment
STM ΔlsrB

769 **Fig. 6 LuxS/AI-2 signaling regulates critical gene targets to assist in multiple**
770 **stages of *Salmonella* infection in the host.** Transcriptomic analysis of STM WT,
771 STM *ΔluxS*, STM *ΔlsrB*, and STM *ΔlsrK* grown in LB media **(A-C)**. Gene
772 enrichment (GO) and KEGG analysis in STM *ΔluxS* and STM *ΔlsrB* **(D-E).**
773

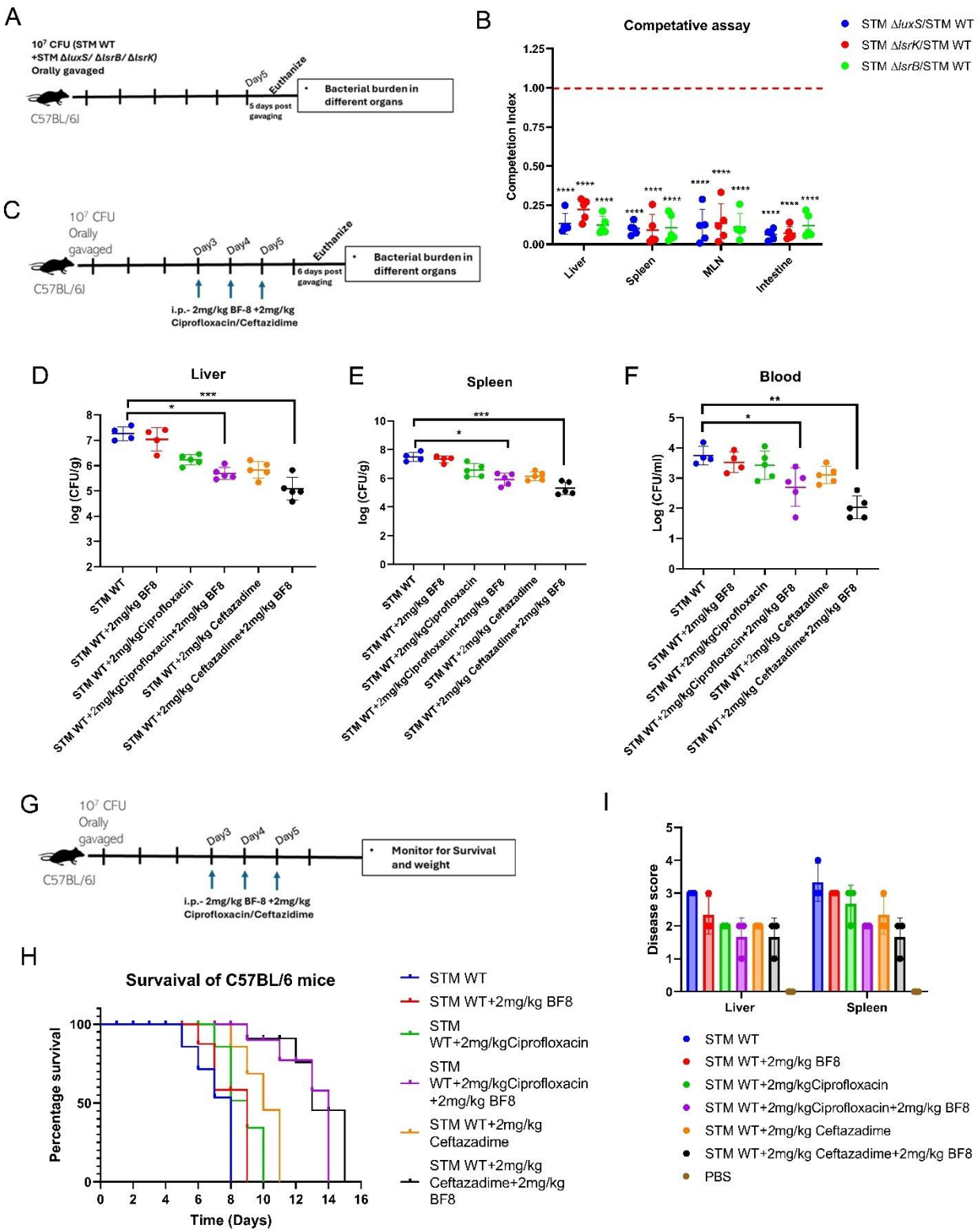

774

775

776 **Fig. 7 Inhibition of LuxS/AI-2 signaling with antibiotics reduces *Salmonella***

777 **colonization *in vivo* and enhances mice survival. (A)** The Competitive

experimental protocol for organ burden in C57BL/6J mice by orally gavaging a total of 10^7 CFU per mouse. **(B)**The organ burden post 5 days of oral gavage in a competition assay. Represented as Mean+/-SD of N=2, n=5 **(C)**. The experimental protocol for C57BL/6J mice infected with STM WT by orally gavaging 10^7 and BF-8 and an antibiotic treatment. Organ burden post treatment **(D)** Liver, (**E)** Spleen, and **(F)** Blood. Represented as Mean+/-SD of N=2, n=5. **(G)** The experimental protocol of mouse survival in C57BL/6J mice involved orally gavaging 10^7 CFU per mouse upon treatment with the BF-8 inhibitor and a combination of antibiotics (through the Intraperitoneal route). **(H)** Percentage survival of Mice upon infection with STM WT with and without treatment. **(I)** Disease score from the histopathological sections of the liver and spleen. Non-parametric One-way ANOVA (Kruskal-Wallis) with Dunn's post hoc test was used to analyze organ burden in mice.

References -

1. Nealson KH, Platt T, Hastings JW. Cellular control of the synthesis and activity of the bacterial luminescent system. Journal of bacteriology. 1970;104(1):313-22.
2. Fuqua WC, Winans SC, Greenberg EP. Quorum sensing in bacteria: the LuxR-LuxI family of cell density-responsive transcriptional regulators. Journal of bacteriology. 1994;176(2):269-75.
3. Bassler BL, Wright M, Showalter RE, Silverman MR. Intercellular signalling in Vibrio harveyi: sequence and function of genes regulating expression of luminescence. Molecular microbiology. 1993;9(4):773-86.
4. Taga ME, Bassler BL. Chemical communication among bacteria. Proceedings of the National Academy of Sciences. 2003;100(suppl_2):14549-54.
5. Asad S, Opal SM. Bench-to-bedside review: quorum sensing and the role of cell-to-cell communication during invasive bacterial infection. Critical care. 2008;12(6):236.
6. Greenberg EP. Bacterial communication and group behavior. The Journal of clinical investigation. 2003;112(9):1288-90.
7. Miller MB, Bassler BL. Quorum sensing in bacteria. Annual Reviews in Microbiology. 2001;55(1):165-99.
8. Ikuta KS, Swetschinski LR, Aguilar GR, Sharara F, Mestrovic T, Gray AP, et al. Global mortality associated with 33 bacterial pathogens in 2019: a systematic analysis for the Global Burden of Disease Study 2019. The Lancet. 2022;400(10369):2221-48.
9. Hajra D, Nair AV, Chakravortty D. Decoding the invasive nature of a tropical pathogen of concern: The invasive non-Typhoidal Salmonella strains causing host-restricted extraintestinal infections worldwide. Microbiological Research. 2023;277:127488.
10. Marcus SL, Brumell JH, Pfeifer CG, Finlay BB. Salmonella pathogenicity islands: big virulence in small packages. Microbes and infection. 2000;2(2):145-56.
11. Pradhan D, Devi Negi V. Stress-induced adaptations in Salmonella: A ground for shaping its pathogenesis. Microbiol Res. 2019;229:126311.
12. Gal-Mor O. Persistent Infection and Long-Term Carriage of Typhoidal and Nontyphoidal Salmonellae. Clin Microbiol Rev. 2019;32(1).
13. Fabrega A, Vila J. Salmonella enterica serovar Typhimurium skills to succeed in the host: virulence and regulation. Clin Microbiol Rev. 2013;26(2):308-41.
14. Miller MB, Bassler BL. Quorum sensing in bacteria. Annu Rev Microbiol. 2001;55:165-99.
15. Walters M, Sperandio V. Quorum sensing in Escherichia coli and Salmonella. Int J Med Microbiol. 2006;296(2-3):125-31.
16. Sholpan A, Lamas A, Cepeda A, Franco CM. Salmonella spp. quorum sensing: an overview from environmental persistence to host cell invasion. AIMS Microbiol. 2021;7(2):238-56.
17. Rezzonico F, Smits TH, Duffy B. Detection of AI-2 receptors in genomes of Enterobacteriaceae suggests a role of type-2 quorum sensing in closed ecosystems. Sensors (Basel). 2012;12(5):6645-65.
18. Miller ST, Xavier KB, Campagna SR, Taga ME, Semmelhack MF, Bassler BL, et al. Salmonella typhimurium recognizes a chemically distinct form of the bacterial quorum-sensing signal AI-2. Mol Cell. 2004;15(5):677-87.
19. Vendeville A, Winzer K, Heurlier K, Tang CM, Hardie KR. Making 'sense' of metabolism: autoinducer-2, LuxS and pathogenic bacteria. Nat Rev Microbiol. 2005;3(5):383-96.
20. Chatterjee R, Shreenivas MM, Sunil R, Chakravortty D. Enteropathogens: Tuning Their Gene Expression for Hassle-Free Survival. Frontiers in microbiology. 2018;9:3303.
21. Choi J, Shin D, Kim M, Park J, Lim S, Ryu S. LsrR-mediated quorum sensing controls invasiveness of Salmonella typhimurium by regulating SPI-1 and flagella genes. PloS one. 2012;7(5):e37059.

22. Choi J, Park J, Ryu S. Repressed Quorum sensing by overexpressing LsrR Hampers Salmonella evasion from oxidative killing within macrophages. Journal of microbiology and biotechnology. 2010;20(12):1624-9.
23. Wang Y, Liu B, Grenier D, Yi L. Regulatory Mechanisms of the LuxS/AI-2 System and Bacterial Resistance. Antimicrobial agents and chemotherapy. 2019;63(10).
24. Laganenka L, Colin R, Sourjik V. Chemotaxis towards autoinducer 2 mediates autoaggregation in Escherichia coli. Nat Commun. 2016;7:12984.
25. Laganenka L, Lee JW, Malfertheiner L, Dieterich CL, Fuchs L, Piel J, et al. Chemotaxis and autoinducer-2 signalling mediate colonization and contribute to co-existence of Escherichia coli strains in the murine gut. Nat Microbiol. 2023;8(2):204-17.
26. Ismail AS, Valastyan JS, Bassler BL. A Host-Produced Autoinducer-2 Mimic Activates Bacterial Quorum Sensing. Cell Host Microbe. 2016;19(4):470-80.
27. Hegde M, Englert DL, Schrock S, Cohn WB, Vogt C, Wood TK, et al. Chemotaxis to the quorum-sensing signal AI-2 requires the Tsr chemoreceptor and the periplasmic LsrB AI-2-binding protein. Journal of bacteriology. 2011;193(3):768-73.
28. Rodrigues MV, Ferreira A, Ramirez-Montoya M, Oliveira RA, Defaix R, Kis P, et al. Manipulation and quantification of the levels of Autoinducer-2 quorum sensing signal in the mouse gut. Bioorg Chem. 2025;157:108274.
29. Datsenko KA, Wanner BL. One-step inactivation of chromosomal genes in Escherichia coli K-12 using PCR products. Proceedings of the National Academy of Sciences of the United States of America. 2000;97(12):6640-5.
30. Janssens JC, Steenackers H, Robijns S, Gellens E, Levin J, Zhao H, et al. Brominated furanones inhibit biofilm formation by Salmonella enterica serovar Typhimurium. Appl Environ Microbiol. 2008;74(21):6639-48.
31. Pan J, Bahar AA, Syed H, Ren D. Reverting antibiotic tolerance of Pseudomonas aeruginosa PAO1 persister cells by (Z)-4-bromo-5-(bromomethylene)-3-methylfuran-2(5H)-one. PloS one. 2012;7(9):e45778.
32. Simon Andrews F, Segonds-Pichon A, Biggins L, Krueger C, Wingett S. FastQC: a quality control tool for high throughput sequence data. 2010.
33. Chen S. Ultrafast one-pass FASTQ data preprocessing, quality control, and deduplication using fastp. Imeta. 2023;2(2):e107.
34. Kopylova E, Noé L, Touzet H. SortMeRNA: fast and accurate filtering of ribosomal RNAs in metatranscriptomic data. Bioinformatics. 2012;28(24):3211-7.
35. Kim D, Paggi JM, Park C, Bennett C, Salzberg SL. Graph-based genome alignment and genotyping with HISAT2 and HISAT-genotype. Nature biotechnology. 2019;37(8):907-15.
36. Liao Y, Smyth GK, Shi W. featureCounts: an efficient general purpose program for assigning sequence reads to genomic features. Bioinformatics. 2014;30(7):923-30.
37. Love MI, Huber W, Anders S. Moderated estimation of fold change and dispersion for RNA-seq data with DESeq2. Genome biology. 2014;15(12):550.
38. Garai P, Lahiri A, Ghosh D, Chatterjee J, Chakravortty D. Peptide utilizing carbon starvation gene yjiY is required for flagella mediated infection caused by Salmonella. Microbiology. 2016;162(1):100-16.
39. Nair AV, Singh A, Devasurmutt Y, Rahman SA, Tatu US, Chakravortty D. Spermidine constitutes a key determinant of Motility and attachment of Salmonella Typhimurium through a novel regulatory mechanism. Microbiol Res. 2024;281:127605.
40. Toker AS, Macnab RM. Distinct regions of bacterial flagellar switch protein FliM interact with FliG, FliN and CheY. J Mol Biol. 1997;273(3):623-34.
41. Sarkar MK, Paul K, Blair D. Chemotaxis signaling protein CheY binds to the rotor protein FliN to control the direction of flagellar rotation in Escherichia coli. Proceedings of the National Academy of Sciences of the United States of America. 2010;107(20):9370-5.

42. Aizawa S-I, Minamino T. Flagella. Molecular medical microbiology: Elsevier; 2024. p. 97-126.
43. Frye J, Karlinsey JE, Felise HR, Marzolf B, Dowidar N, McClelland M, et al. Identification of new flagellar genes of Salmonella enterica serovar Typhimurium. Journal of bacteriology. 2006;188(6):2233-43.
44. Mukherjee S, Bassler BL. Bacterial quorum sensing in complex and dynamically changing environments. Nat Rev Microbiol. 2019;17(6):371-82.
45. Kim MK, Ingremeau F, Zhao A, Bassler BL, Stone HA. Local and global consequences of flow on bacterial quorum sensing. Nat Microbiol. 2016;1:15005.
46. Millet YA, Alvarez D, Ringgaard S, von Andrian UH, Davis BM, Waldor MK. Insights into Vibrio cholerae intestinal colonization from monitoring fluorescently labeled bacteria. PLoS pathogens. 2014;10(10):e1004405.
47. Zhao X, Koestler BJ, Waters CM, Hammer BK. Post-transcriptional activation of a diguanylate cyclase by quorum sensing small RNAs promotes biofilm formation in Vibrio cholerae. Mol Microbiol. 2013;89(5):989-1002.
48. Carter PB, Collins FM. The route of enteric infection in normal mice. The Journal of experimental medicine. 1974;139(5):1189-203.
49. Niemann HH, Schubert WD, Heinz DW. Adhesins and invasins of pathogenic bacteria: a structural view. Microbes and infection. 2004;6(1):101-12.
50. Pizarro-Cerda J, Cossart P. Bacterial adhesion and entry into host cells. Cell. 2006;124(4):715-27.
51. Cooper KG, Kari L, Chong A, Tandon N, Doran K, Gomes Da Silva L, et al. HilD-regulated chemotaxis proteins contribute to Salmonella Typhimurium colonization in the gut. mBio. 2025;16(4):e0039025.
52. Cooper KG, Chong A, Kari L, Jeffrey B, Starr T, Martens C, et al. Regulatory protein HilD stimulates Salmonella Typhimurium invasiveness by promoting smooth swimming via the methyl-accepting chemotaxis protein McpC. Nat Commun. 2021;12(1):348.
53. Muniz LR, Knosp C, Yeretssian G. Intestinal antimicrobial peptides during homeostasis, infection, and disease. Frontiers in immunology. 2012;3:310.
54. Singh A, Nair AV, Aroli S, Das S, Karmakar S, Mukherjee S, et al. LuxS/AI-2 signaling in Salmonella Typhimurium regulates phoP/phoQ to protect against acidic pH for enhanced survival in macrophages. bioRxiv. 2025:2025.03. 26.645541.
55. Gunn JS, Miller SI. PhoP-PhoQ activates transcription of pmrAB, encoding a two-component regulatory system involved in Salmonella typhimurium antimicrobial peptide resistance. Journal of bacteriology. 1996;178(23):6857-64.
56. Shprung T, Peleg A, Rosenfeld Y, Trieu-Cuot P, Shai Y. Effect of PhoP-PhoQ activation by broad repertoire of antimicrobial peptides on bacterial resistance. The Journal of biological chemistry. 2012;287(7):4544-51.
57. Richards SM, Strandberg KL, Conroy M, Gunn JS. Cationic antimicrobial peptides serve as activation signals for the Salmonella Typhimurium PhoPQ and PmrAB regulons in vitro and in vivo. Front Cell Infect Microbiol. 2012;2:102.
58. Shprung T, Wani NA, Wilmes M, Mangoni ML, Bitler A, Shimoni E, et al. Opposing Effects of PhoPQ and PmrAB on the Properties of Salmonella enterica serovar Typhimurium: Implications on Resistance to Antimicrobial Peptides. Biochemistry. 2021;60(39):2943-55.
59. Shi Y, Latifi T, Cromie MJ, Groisman EA. Transcriptional control of the antimicrobial peptide resistance ugtL gene by the Salmonella PhoP and SlyA regulatory proteins. The Journal of biological chemistry. 2004;279(37):38618-25.
60. Chen HD, Jewett MW, Groisman EA. An allele of an ancestral transcription factor dependent on a horizontally acquired gene product. PLoS Genet. 2012;8(12):e1003060.

61. McPhee JB, Bains M, Winsor G, Lewenza S, Kwasnicka A, Brazas MD, et al. Contribution of the PhoP-PhoQ and PmrA-PmrB two-component regulatory systems to Mg2+-induced gene regulation in Pseudomonas aeruginosa. Journal of bacteriology. 2006;188(11):3995-4006.
62. Groisman EA. The pleiotropic two-component regulatory system PhoP-PhoQ. Journal of bacteriology. 2001;183(6):1835-42.
63. Galan JE. Salmonella Typhimurium and inflammation: a pathogen-centric affair. Nat Rev Microbiol. 2021;19(11):716-25.
64. Haraga A, Ohlson MB, Miller SI. Salmonellae interplay with host cells. Nat Rev Microbiol. 2008;6(1):53-66.
65. Nair AV, Singh A, Rajmani RS, Chakravortty D. Salmonella Typhimurium employs spermidine to exert protection against ROS-mediated cytotoxicity and rewires host polyamine metabolism to ameliorate its survival in macrophages. Redox Biol. 2024;72:103151.
66. Ha JH, Hauk P, Cho K, Eo Y, Ma X, Stephens K, et al. Evidence of link between quorum sensing and sugar metabolism in Escherichia coli revealed via cocrystal structures of LsrK and HPr. Science advances. 2018;4(6):eaar7063.
67. Oliveira RA, Cabral V, Torcato I, Xavier KB. Deciphering the quorum-sensing lexicon of the gut microbiota. Cell Host Microbe. 2023;31(4):500-12.
68. Thompson JA, Oliveira RA, Djukovic A, Ubeda C, Xavier KB. Manipulation of the quorum sensing signal AI-2 affects the antibiotic-treated gut microbiota. Cell reports. 2015;10(11):1861-71.
69. Lagkouvardos I, Lesker TR, Hitch TC, Gálvez EJ, Smit N, Neuhaus K, et al. Sequence and cultivation study of Muribaculaceae reveals novel species, host preference, and functional potential of this yet undescribed family. Microbiome. 2019;7:1-15.
70. Hegde M, Englert DL, Schrock S, Cohn WB, Vogt C, Wood TK, et al. Chemotaxis to the quorum-sensing signal AI-2 requires the Tsr chemoreceptor and the periplasmic LsrB AI-2-binding protein. Journal of bacteriology. 2011;193(3):768-73.
71. Shprung T, Peleg A, Rosenfeld Y, Trieu-Cuot P, Shai Y. Effect of PhoP-PhoQ activation by broad repertoire of antimicrobial peptides on bacterial resistance. Journal of Biological Chemistry. 2012;287(7):4544-51.
72. McPhee JB, Bains M, Winsor G, Lewenza S, Kwasnicka A, Brazas MD, et al. Contribution of the PhoP-PhoQ and PmrA-PmrB two-component regulatory systems to Mg2+-induced gene regulation in Pseudomonas aeruginosa. Journal of bacteriology. 2006;188(11):3995-4006.
73. Molloy MJ, Grainger JR, Bouladoux N, Hand TW, Koo LY, Naik S, et al. Intraluminal containment of commensal outgrowth in the gut during infection-induced dysbiosis. Cell Host Microbe. 2013;14(3):318-28.
74. Haag LM, Fischer A, Otto B, Plickert R, Kuhl AA, Gobel UB, et al. Intestinal microbiota shifts towards elevated commensal Escherichia coli loads abrogate colonization resistance against Campylobacter jejuni in mice. PloS one. 2012;7(5):e35988.